

X-RAY OBSERVATIONS OF THE SUPERNOVA REMNANT N103B IN THE LARGE MAGELLANIC CLOUD

K. P. SINGH,¹ N. J. WESTERGAARD, AND H. W. SCHNOPPER
 Danish Space Research Institute, Lyngby, Denmark

AND

D. J. HELFAND

Columbia Astrophysics Laboratory, Columbia University

Received 1986 August 28; accepted 1987 April 24

ABSTRACT

We present X-ray observations of the supernova remnant N103B made with both the low-energy and medium-energy experiments on board *EXOSAT*. Fitting the spectral data obtained from *EXOSAT* and from the *Einstein Observatory* with thermal models yields satisfactory fits for a temperature of ~ 1.2 keV, while power-law models appear to be excluded. The X-ray luminosity of N103B is 1.6×10^{37} ergs s^{-1} in the 0.05–4.5 keV energy band. The X-ray emission as seen in the low-energy telescope on *EXOSAT* is centrally peaked. The upper limit on its extent in soft X-rays derived from this experiment is $\sim 25''$, which is comparable to its optical size. The spatial resolution of the present observations is not sufficient to discern the morphology of X-ray emission from N103B. Its small diameter and high luminosity suggest that it is quite young (600–1200 yr). The failure of power-law models to explain the spectral data on N103B suggests that, despite its centrally peaked surface brightness distribution, its resemblance to a Crab-like supernova remnant is only superficial. A central source with “Crab-like” nonthermal X-ray luminosity of up to 6×10^{35} ergs s^{-1} is, however, allowed by the spectral data.

Subject headings: galaxies: Magellanic Clouds — nebulae: supernova remnants — X-rays: sources — X-rays: spectra

I. INTRODUCTION

The supernova remnant N103B is one of the brightest radio and X-ray supernova remnants in the Large Magellanic Cloud (Long, Helfand, and Grabelsky 1981; Mathewson *et al.* 1983; Mills *et al.* 1984). It was first identified as a supernova remnant (SNR) by Mathewson and Clarke (1973) based on the non-thermal nature of its radio spectrum and the relative emission-line strengths of [S II] and H α . Its radio spectral index of -0.53 is typical of shell-type remnants (e.g., Kepler, Tycho, Cygnus Loop, and N132D in the LMC). However, this source is unresolved in the radio with a size of <0.4 (Mills *et al.* 1984). Its X-ray map obtained with the High Resolution Imager on the *Einstein Observatory* shows a centrally peaked brightness distribution with an extent of $\sim 25''$ (Mathewson *et al.* 1983). Its optical image in the light of H α shows four bright knots of emission (Mathewson *et al.* 1983). Its size given by Mathewson *et al.* is $23'' \times 18''$, which, at a distance of 55 kpc, corresponds to a diameter of ~ 6 pc.

We report here new X-ray observations of N103B made using the European X-Ray Observatory satellite *EXOSAT* and the *Einstein Observatory*. An X-ray map from *EXOSAT* obtained with three different filters corresponding to three different energy bands is presented. The analysis of the X-ray spectra obtained from both *EXOSAT* and the *Einstein Observatory* indicates a thermal origin for X-rays from N103B. We begin by describing the observations (§ II) and then present an analysis of the spectral data (§ III). In § IV, we discuss what can be inferred regarding the remnant’s age and evolutionary state, concluding (§ V) with a summary of our results.

II. OBSERVATIONS

a) EXOSAT

A 10.5 hr exposure centered on N103B [$\alpha(1950) = 05^{\text{h}}09^{\text{m}}12^{\text{s}}$, $\delta(1950) = -68^{\circ}47'12''$] was made with *EXOSAT* on day 320 of 1984. The observations were performed with the medium-energy (ME) experiment (Turner, Smith, and Zimmerman 1981) and the low-energy (LE) experiment (de Korte *et al.* 1981). The ME experiment consists of eight proportional counters with a total geometric area of $\sim 1500 \text{ cm}^2$ and a field of view of $45' \times 45'$ (FWHM). Each detector has an argon-filled chamber in front which is sensitive in the energy range 1.5–20 keV and a rear xenon-filled chamber sensitive in the 5–50 keV energy range. The instrument is divided into four quadrants of two detectors each. During this exposure two quadrants were coaligned and pointed at N103B, while the other two quadrants were offset by $113'$ (the maximum offset allowed is $132'$). One of the offset quadrants pointed at $\alpha = 05^{\text{h}}02^{\text{m}}57.6$, $\delta = -76^{\circ}36'00''$ and the other at $\alpha = 04^{\text{h}}51^{\text{m}}21.6$, $\delta = -68^{\circ}07'12''$. The contribution of the off-axis weak Large Magellanic Cloud sources (see Long, Helfand, and Grabelsky 1981) present in the field of view (FOV) of these detectors is negligible, and the data from these detectors were used as a monitor of background. After $\sim 20,800$ s of the observation, the offset quadrants were moved to point at N103B, and the other two quadrants were offset by $76'$. The new offset view directions were $\alpha = 05^{\text{h}}23^{\text{m}}49^{\text{s}}2$, $\delta = -69^{\circ}09'36''$ and $\alpha = 05^{\text{h}}14^{\text{m}}48^{\text{s}}$, $\delta = -67^{\circ}34'12''$. The quadrant pointed toward the latter position effectively looked at blank sky and provided a good background monitor. The other quadrant, however, had the strong source N132D in its FOV about $40'$ off-axis, where the detection efficiency is about 8% of the peak. Since

¹ On leave from Tata Institute of Fundamental Research, Bombay, India.

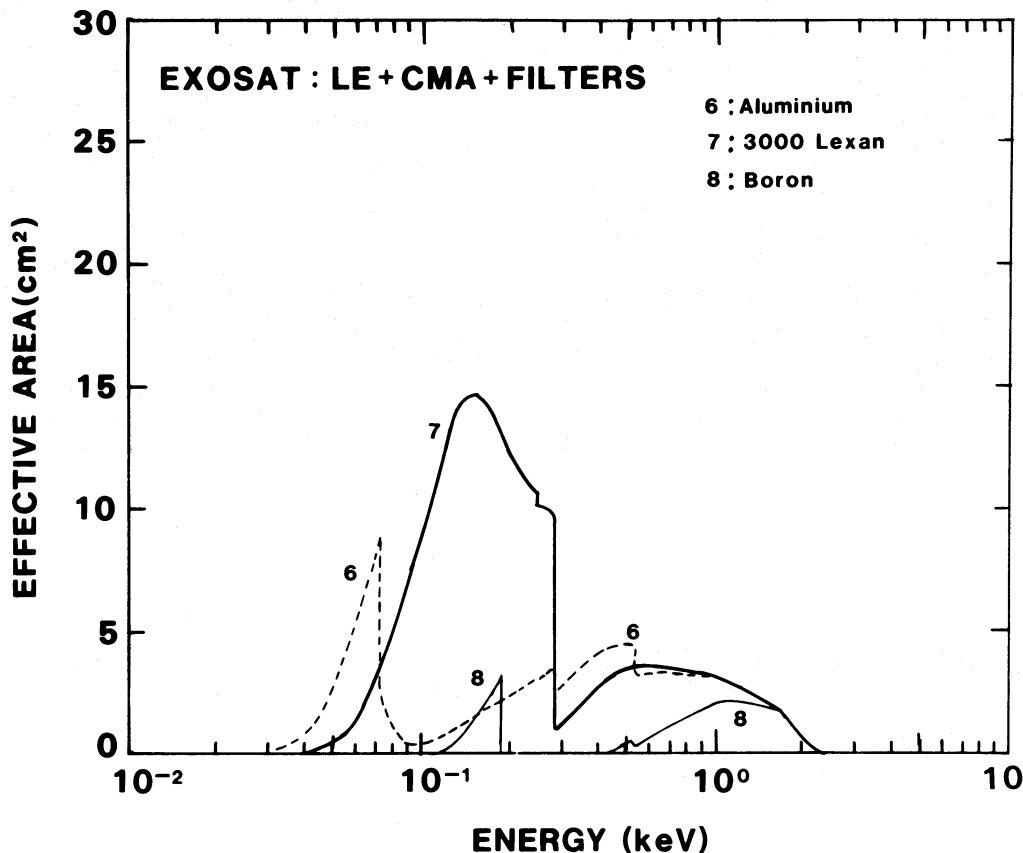


FIG. 1.—Efficiency of the channel multiplier array (CMA) together with three different filters and the low-energy (LE) telescope on *EXOSAT*

data from both offset quadrants are combined for use as a background subtraction from the earlier pointed observation by these detectors, the net contamination from N132D is only 4%. N132D is about 4 times brighter than N103B, and this causes an oversubtraction of about 16% of the N103B flux in these four detectors. A useful exposure of about 30,350 s was obtained after removing the data coincident with transient background events. A simultaneous observation with the LE experiment pointed at N103B showed no other sources detectable in the ME field of view. After applying the correction due to the oversubtraction, the average count rate detected from N103B in the argon-filled counters is 0.99 counts s^{-1} . This rate is consistent with the apparent lack of detectable counts in the xenon chambers.

The soft X-ray observations of N103B were carried out with the channel multiplier array (CMA) together with three different filters at the focus of the LE telescope. The combined efficiency of the LE + CMA + each filter used is shown in Figure 1. The response of the LE + CMA with the 3000 Å Lexan (3LX) filter is the broadest (0.04–2.0 keV). The other two filters, aluminum/parylene (Al/P) and boron, have their widest transmission bands in the energy ranges 0.1–2.0 keV and 0.5–2.0 keV, respectively. These filters also have lower efficiency transmission bands at 0.03–0.09 keV for the aluminum filter and at 0.14–0.19 keV for the boron filter. The useful exposures and the average count rates obtained from each of the three filters are listed in Table 1. The count rates have been corrected for the shadowing of the field of view by the ME “flap,” the sum signal distribution, the telemetry dead time, and the vignetting in the LE telescope (Osborne 1985). The total numbers of photons

detected from the source with each of the three filters are comparable.

In Figures 2a–2c we show the contour maps of the X-ray surface brightness of N103B obtained with each of the three filters. The maps have been smoothed with a Gaussian of $FWHM = 23.5''$, which is comparable to the point-spread function obtained from observations with Cyg X-2 in the center of the field of view of the LE telescope plus the 3LX filter. The three images seem to show small differences in their brightness distributions. The boron and Al/P filter images (similar energy bandpasses) show similarly oriented elliptical shapes which differ from the image obtained using the 3LX filter with its softer energy response. The differences are, however, not statistically significant because of the inherent ellipticity in the point-spread function of the telescope and the differences in X-ray scattering by each of the three filters (particularly in the boron filter; see Davelaar and Giommi 1985). In fact, with the present statistics in the images, it is not possible to distinguish between a point source and a ringlike source of $\sim 20''$ diameter (comparable to the optical size of N103B). By assuming azi-

TABLE 1
EXOSAT LE + CMA OBSERVATIONS OF N103B

Filter Name	Exposure Time (s)	Corrected Count Rate (counts s^{-1})
3000 Lexan	6560	0.035 ± 0.003
Boron + polypropylene	17413	0.010 ± 0.001
Aluminum/parylene	5947	0.023 ± 0.0026

mutual symmetry and using the counting statistics from the 3LX image, we find the FWHM of the image size to be approximately $28'' \pm 4.5''$, which, for a point-spread function of $24''$, places an upper limit (2σ) of $\sim 25''$ on the source size.

b) Einstein Observatory

As a part of the X-ray survey of the Large Magellanic Cloud (Long, Helfand, and Grabelsky 1981) with the imaging proportional counter (IPC) on board the *Einstein Observatory* (Giacconi *et al.* 1979), N103B was observed for 2320 s on day 205 of 1979. The supernova remnant N103B was detected with a count rate of 0.80 ± 0.02 counts s^{-1} in the energy range 0.2–3.5 keV. The count rate has been corrected for vignetting, mirror scattering, and instrument dead-time effects. The radial distribution of the X-ray photons observed from this source is indistinguishable from that of a point source, indicating that the extent of the source is smaller than $1'$.

The High Resolution Imager (HRI) map published by Mathewson *et al.* (1983) shows a strong central peak and a total extent of $25''$. An examination of the reprocessed HRI data has, however, revealed that there is a serious aspect problem associated with this observation, arising from the fact that the guide star is embedded in substantial nebulosity. Typical aspect solution errors are $10''$ – $16''$ throughout the observation. Since there is no pointlike X-ray source within the

HRI field of view, a *post hoc* aspect has proved impossible. The true X-ray extent of the source, then, is smaller than that indicated in Figure 7b of Mathewson *et al.* (1983). Although the X-ray contours in the figure indicate emission approximately coextensive with the optical knots, this result should be viewed with extreme caution; the size limit of $\leq 25''$ derived from our *EXOSAT* observation is perhaps the most secure value of the remnant's diameter in the soft X-ray band.

III. THE X-RAY SPECTRUM OF N103B

The combined background-subtracted argon chamber pulse-height (PH) spectrum for the eight detectors of the ME experiment together with the count rates obtained from the LE experiment on the *EXOSAT* are shown in Figure 3. Both power-law and thermal bremsstrahlung (exponential plus Gaunt factor) models together with a low-energy absorption term were used to fit the observed PH distribution from the ME experiment and the count rates from the LE experiment. The data are better fitted with a thermal model ($\chi^2 = 20.4$ for 11 degrees of freedom) than with a nonthermal model ($\chi^2 = 25.5$ for 11 degrees of freedom), which required a photon index $\gtrsim 4$. The best-fit thermal model has $kT = 1.2$ keV, $N_H = 7.5 \times 10^{20}$ atoms cm^{-2} , and normalization constant = 1.1×10^{-2} photons $cm^{-2} s^{-1} keV^{-1}$. This model is shown as a histogram in Figure 3a. Using the model of

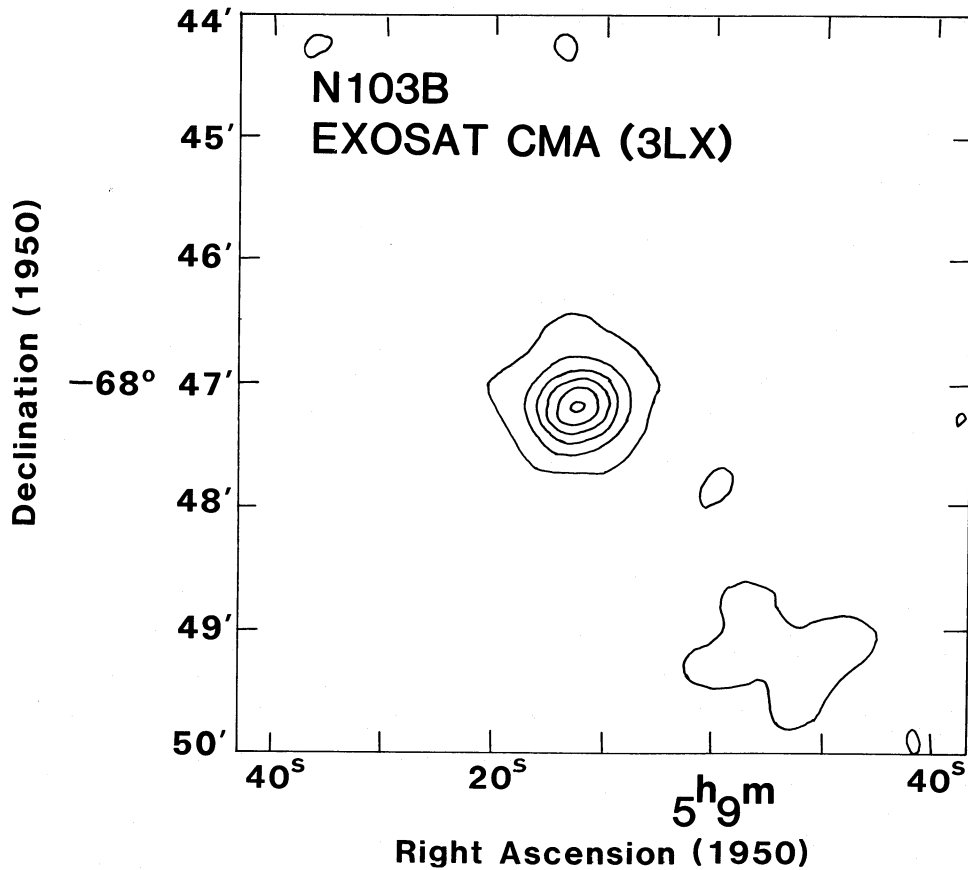
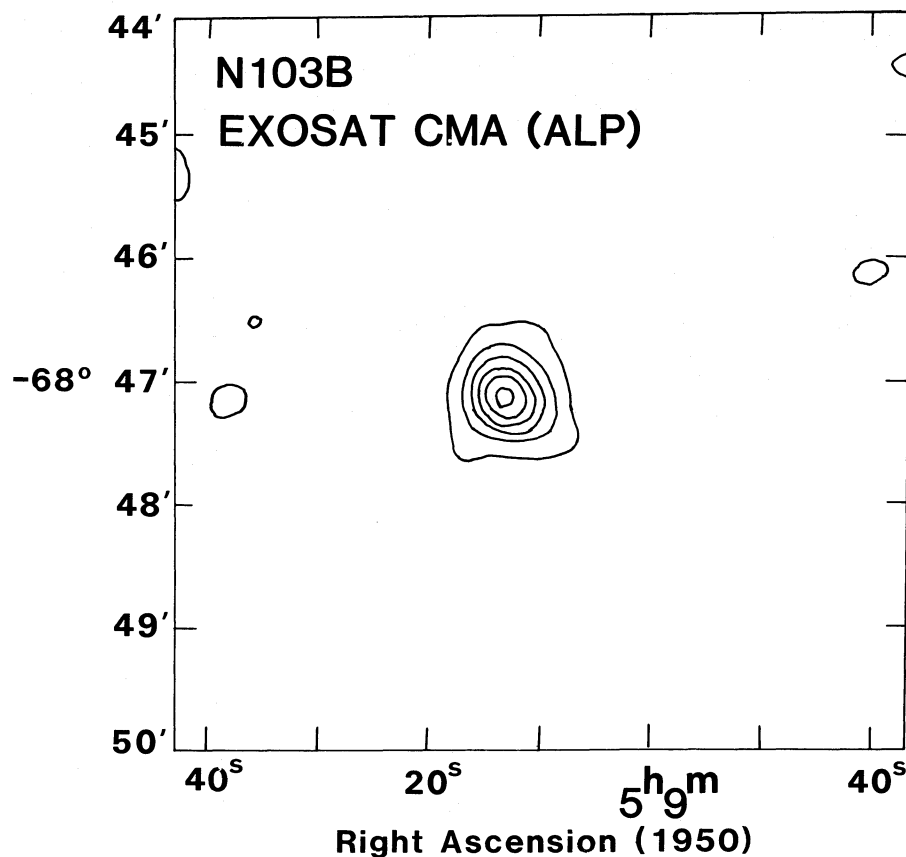


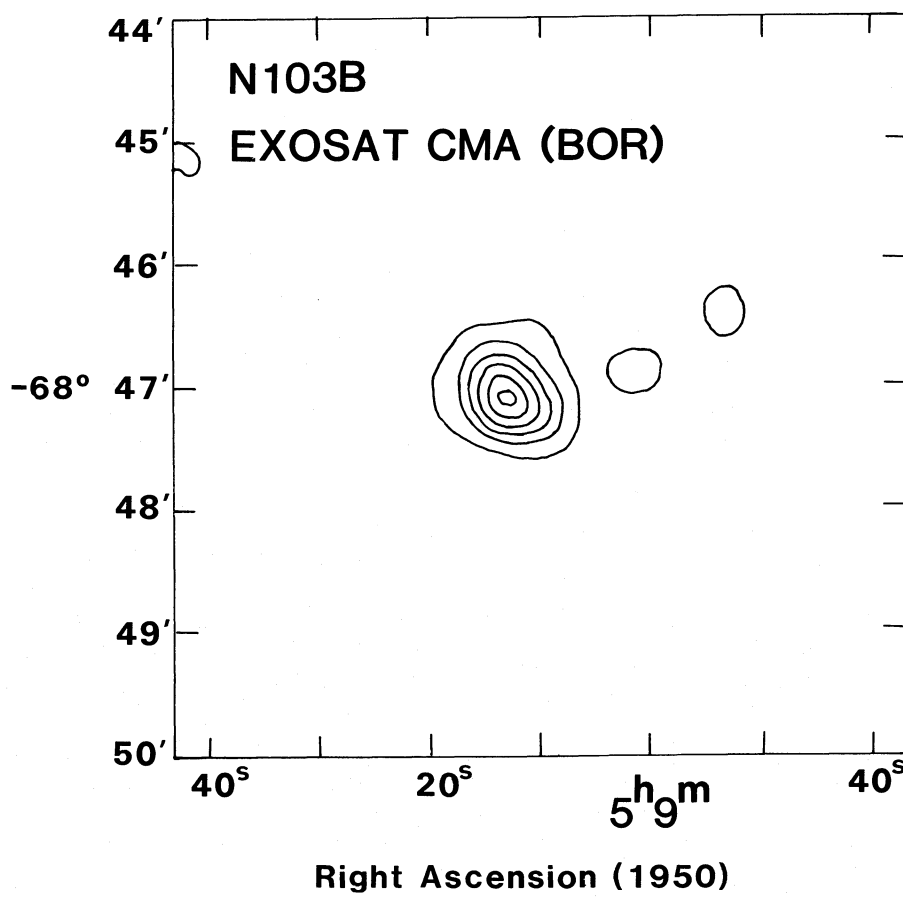
FIG. 2a

FIG. 2.—(a) Soft X-ray image of the N103B obtained with the LE telescope + 3LX filter on *EXOSAT*. The image has been smoothed with a Gaussian function of $10''$ standard deviation. The contour levels are 0.2, 0.58, 0.96, 1.36, 1.72, and 2.1 counts per pixel of $4'' \times 4''$ size. (b) Same as (a), for the Al/P filter. The contour levels are 0.2, 0.4, 0.6, 0.8, 1.0, and 1.2 counts per pixel of $4'' \times 4''$ size. (c) Same as (a), for the boron filter. The contour levels are 0.3, 0.56, 0.82, 1.34, and 1.6 counts per pixel of $4'' \times 4''$ size.

Declination (1950)



Declination (1950)



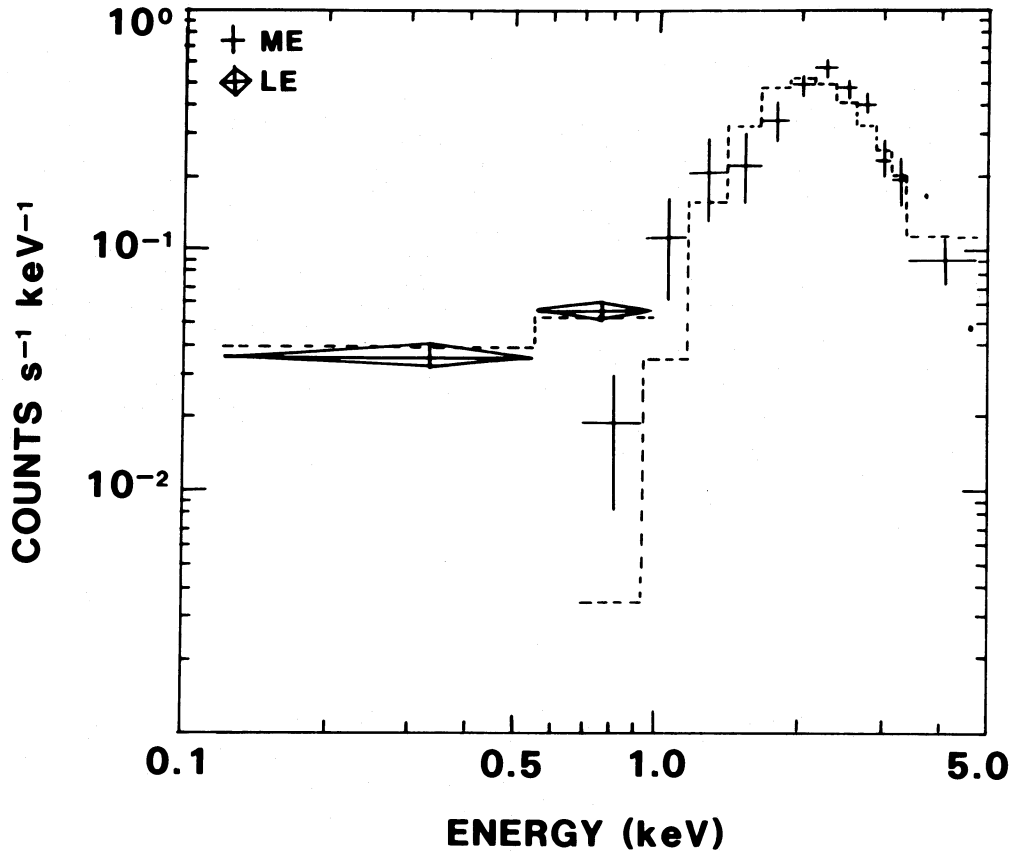


FIG. 3a

FIG. 3.—(a) X-ray pulse-height spectrum from ME observations of N103B. The counts observed with the LE telescope are also shown. The histogram shows the predicted count rates for the best-fit thermal model. (b) X-ray pulse-height spectrum of N103B from the IPC observation. The predicted count rates from the best-fit thermal model are shown as a histogram.

Raymond and Smith (1977) for X-ray emission from an optically thin plasma did not improve the fits obtained with our thermal model, and similar values for the parameters kT and N_{H} were deduced. The 90% and 99% confidence contours for kT and N_{H} derived for the thermal bremsstrahlung model using the criterion of Lampton, Margon, and Bowyer (1976) are shown in Figure 4.

The pulse-height spectrum of source N103B was also obtained from the IPC on the *Einstein Observatory* and is shown in Figure 3b. The reprocessed data from the IPC were analyzed for spectral fitting in the energy range 0.2–3.5 keV using the best available energy calibration. Again, nonthermal power-law models as well as Raymond-Smith thermal models together with a low-energy absorption term were used to fit the PH distribution obtained from the IPC. The data were better fitted with a Raymond-Smith thermal model ($\chi^2 = 1.4$ for 7 degrees of freedom) than with a power-law model ($\chi^2 = 17.5$ for 7 degrees of freedom). The 99% confidence contours for kT and N_{H} derived for the Raymond-Smith thermal model, using the criterion of Lampton, Margon, and Bowyer (1976), are shown in Figure 4. The temperature and the N_{H} obtained from fitting these thermal models to the IPC data are consistent with those obtained from the *EXOSAT* data. Furthermore, the higher signal-to-noise ratio in the IPC data rules out the power-law spectrum as an explanation of the PH data from

N103B more convincingly than do the data from the ME + LE experiments on the *EXOSAT*. The best-fit model is shown as a histogram in Figure 3b.

Assuming the best-fit parameters for the thermal emission model obtained from the *EXOSAT* data and adopting a distance of 55 kpc to N103B, we estimate its X-ray luminosity to be 1.7×10^{37} ergs s⁻¹ in the 0.05–4.5 keV energy range. The X-ray luminosity obtained from the IPC count rate using the best-fit parameters for the Raymond-Smith plasma is 1.35×10^{37} ergs s⁻¹ in the 0.2–3.5 keV energy band.

Using the ME data, we have tried to estimate the contribution to the total X-ray flux of N103B from any unresolved nonthermal component in the remnant. We found that fitting two-component spectral models consisting of thermal bremsstrahlung emission plus a power law with photon index (Γ) restricted to the range between 1 and 2 to mimic a Crab-like spectrum led to no further improvement in the minimum χ^2 . An upper limit to the contribution of such a power-law spectrum to the flux from N103B was obtained by adding an increasing power-law component to the best-fit thermal model until χ^2_{min} increased by an unacceptable amount. At 90% confidence, the X-ray luminosity of such a nonthermal component ($\Gamma \sim 2$) in N103B is $< 6.0 \times 10^{35}$ ergs s⁻¹ or $\lesssim 5\%$ of the remnant's total luminosity; this limit decreases as the power-law index hardens.

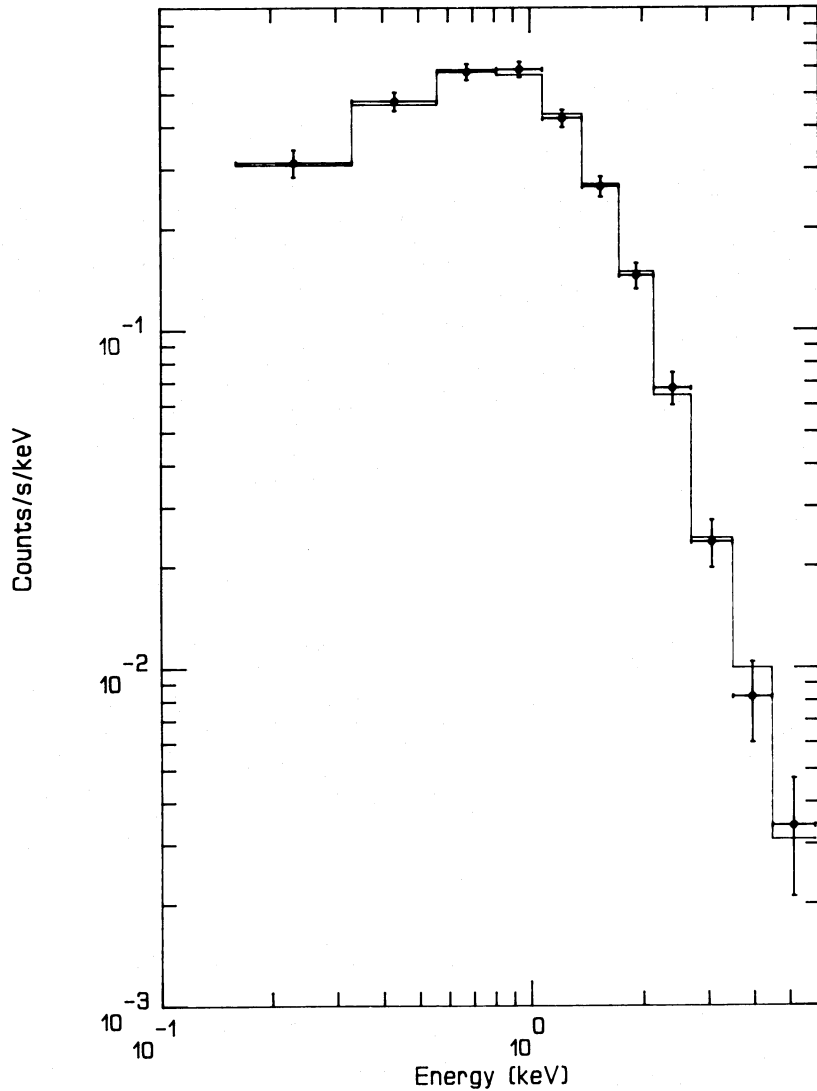


FIG. 3b

IV. APPLICATION OF SNR MODELS

The requirement for the supernova remnant N103B with a radius of 3 pc to yield the observed X-ray luminosity of 1.7×10^{37} ergs s $^{-1}$ in the 0.05–4.5 keV energy band is that the density of the emitting gas must be $n = 7.3\Lambda_{-22}^{-1/2}$ cm $^{-3}$, where Λ_{-22} is the emissivity of the gas in units of 10^{-22} ergs cm 3 s $^{-1}$. For example, McKee and Ostriker (1977) derive $\Lambda = 6.2 \times 10^{-19} T^{-0.6}$ from the calculations of Raymond, Cox, and Smith (1976) for a plasma in ionization equilibrium. For the observed temperature of 1.4×10^7 K, the emissivity for the equilibrium plasma would be 3.2×10^{-23} ergs cm 3 s $^{-1}$ and the calculated density of X-ray-emitting plasma would be increased. If the X-ray-emitting plasma is not in ionization equilibrium, as is very likely if the remnant is very young (see below), then the emissivities are higher than the equilibrium values typically by a factor of 3 (Hamilton, Sarazin, and Chevalier 1983; Masai 1984). The analysis using the nonequilibrium ionization would also give a somewhat different temperature than the one obtained from the use of equilibrium plasma. Furthermore, if we take the emitting gas to have a filling factor f , then the density is increased by the factor $f^{-1/2}$.

Thus, for a density of $7.3f^{-1/2}$ cm $^{-3}$, the total mass of the X-ray gas in the SNR is $\sim 20\Lambda_{-22}^{-1/2} f^{-1/2} M_{\odot}$. The quoted density and the mass of the gas could be higher by as much as a factor of 2 if the plasma emissivities are lower by as much as a factor of 4. The assumption of normal cosmic abundances usually leads to very high estimates of the mass of X-ray-emitting gas (Long, Dopita, and Tuohy 1982). Even if the mass ejected from the progenitor is only $\sim 2 M_{\odot}$, i.e., 10% of the total X-ray mass estimated above from the assumption of cosmic abundances, the effect of enrichment is to lower the estimate of the total X-ray-emitting mass of the SNR to $8 M_{\odot}$ using the prescription of Long, Dopita, and Tuohy (1982).

The age of this remnant and the presupernova ambient gas density around it are unknown. Without a resolved image and kinematic information, it is also difficult to say whether or not N103B is in a free expansion phase or an adiabatic phase. Consequently, the fraction of the mass of the X-ray gas which is due to the swept-up material and the fraction which is supernova ejecta cannot be determined. If, however, the swept-up mass (M_{sw}) is $\gtrsim 10$ times the ejecta mass (M_{ej}), the Sedov relations can be used to estimate certain dynamical parameters

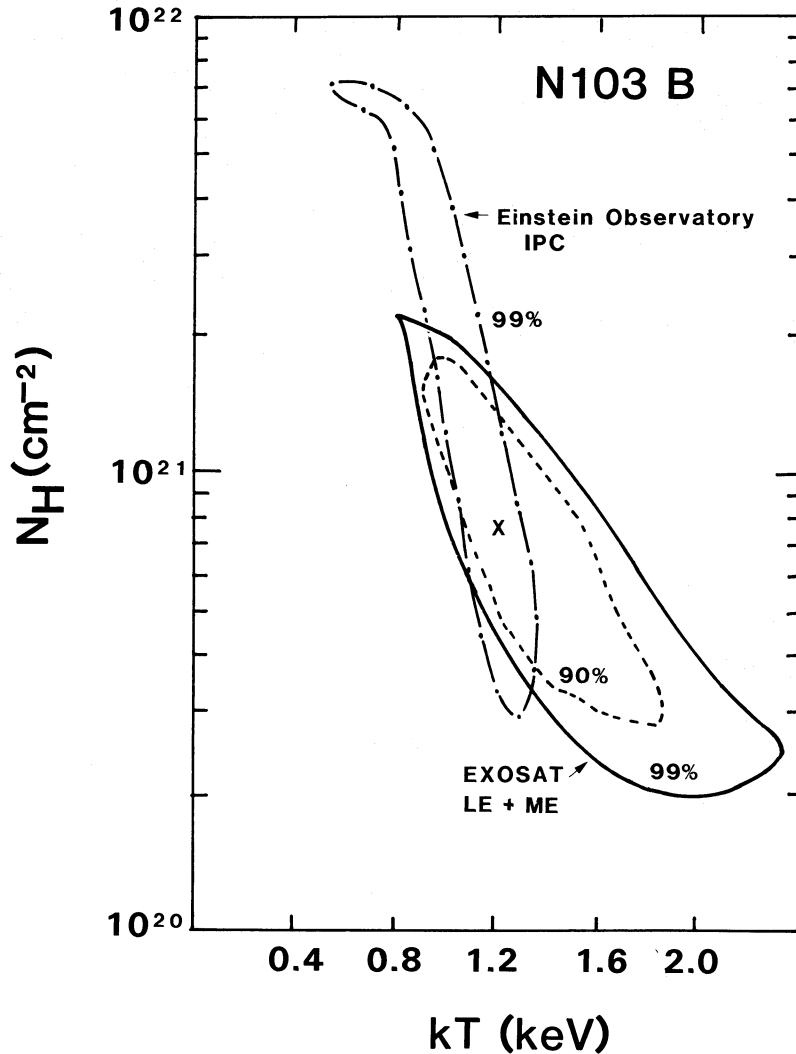


FIG. 4.—The 90% and 99% confidence contours for the thermal models are shown for the EXOSAT ME + LE data. The best-fit values are indicated by a cross. The 99% confidence contour for the thermal models used for fitting the IPC data is also shown.

of N103B. The X-ray luminosity of a Sedov remnant (e.g., Hamilton, Sarazin, and Chevalier 1983) is given by

$$L_x = 3.14 \times 10^{56} n_0^2 r_s^3 \Lambda ,$$

where n_0 is the presupernova ambient gas density in cm^{-3} and r_s is the shock radius in pc. Using the observed radius and X-ray luminosity, we obtain

$$n_0 = 4.50 \Lambda_{22}^{-1/2} \text{ cm}^{-3} . \quad (1a)$$

The shock temperature, age, and shock velocity of the SNR are then given by

$$T_s = 5.25 \times 10^7 \Lambda_{22}^{1/2} E_{51} (r_s/3 \text{ pc})^{-3} \text{ K} , \quad (1b)$$

$$t = 600 \Lambda_{22}^{1/4} E_{51}^{-1/2} (r_s/3 \text{ pc})^{5/2} \text{ yr} , \quad (1c)$$

$$v_s = 1925 \Lambda_{22}^{1/4} E_{51}^{1/2} (r_s/3 \text{ pc})^{-3/2} \text{ km s}^{-1} , \quad (1d)$$

where E_{51} is the supernova explosion energy in units of 10^{51} ergs. From equation (1b), $E_{51} > 0.25$ if the shock temperature is to be at least as high as the observed X-ray temperature of the SNR. The age of N103B would then range between 600 and 1200 yr. The derived parameters indicate a hot, young SNR

that went off in a high-density ambient interstellar medium. Self-consistency with the assumption of Sedov phase requires $n_0 > 4.5 \text{ cm}^{-3}$.

Next, we consider the McKee and Ostriker (1977) model for the evolution of an SNR into a three-phase interstellar medium: the hot low-density phase with $(n, T) \sim (10^{-2.5} \text{ cm}^{-3}, 10^{5.7} \text{ K})$, filling factor 0.7; the cold neutral clouds with $(n, T) \sim (10^{1.6} \text{ cm}^{-3}, 10^{1.9} \text{ K})$, filling factor 0.03; and the warm coronae around the clouds with $T \sim 8000 \text{ K}$ and filling factor ~ 0.25 . Using the parameters for N103B in this model (in particular eqs. [5]–[7] in McKee and Ostriker 1977 and the typical values for the effectiveness of cloud evaporation recommended therein), we obtain for the age of N103B

$$t = 611 E_{51}^{-1/2} \text{ yr} ,$$

in agreement with the value obtained in equation (1c).

The mean expansion velocity for a 600 year old SNR is $r_s/t \approx 5000 \text{ km s}^{-1}$, whereas the shock velocity derived in equation (1d) is only 1925 km s^{-1} , requiring strong deceleration, consistent with the assumption that $M_{\text{sw}} \gg M_{\text{ej}}$.

V. DISCUSSION

The unresolved nature of the radio source in N103B and the suspected center-filled morphology of the remnant in X-rays have led to suggestions that N103B is a "Crab-like" object in which the observed emission is the result of an active neutron star created by the supernova explosion (Mills *et al.* 1984). While the present X-ray imaging data do not rule out the existence of a central source, the predominantly thermal nature of the remnant's X-ray emission suggests that the contribution of such a source to the total luminosity must be small. In fact, the observed X-ray spectrum allows $\lesssim 5\%$ of the total X-ray luminosity to be attributed to a compact nonthermal Crab-like core. The X-ray luminosity of this putative synchrotron component would be only $\sim 5\%$ that of the Crab Nebula but is comparable to that of several other Crab-like remnants (Becker, Helfand, and Szymkowiak 1982).

The bulk of the X-ray emission, however, arises very likely from an extended region $\lesssim 25''$ in diameter which is unresolved by the present observations. This view is consistent with the thermal nature of its X-ray emission, the optical diameter, and the radio spectral index. It is not possible, however, to say whether or not the X-ray emission has a shell morphology, a filled interior, or both. Recent X-ray observations have revealed the existence of a new type of supernova remnant in our Galaxy which has a centrally peaked hot interior and where a soft X-ray shell either is not observed or is not clearly delineated from the interior. Two examples of this remnant type are W44 (Smith *et al.* 1985a) and W49B (Smith *et al.* 1985b). W28 and 3C 400.2 (Matsui and Long 1985) are perhaps similar, but the thermal nature of their X-ray emission has not been confirmed by spectral analysis. These SNRs all have classical radio shells and radio spectral indices of -0.5 . A radio

shell morphology for N103B with $D \lesssim 25''$ is not ruled out, since the radio observations of Mills *et al.* (1984) did not have a sufficient angular resolution to resolve such a shell. Most of these remnants are, however, rather old, large-diameter objects compared with the derived age and size of N103B.

It is also possible that N103B has an X-ray morphology similar to the classical young shell-type remnants (e.g., SN 1006, Kepler, Tycho, or Cas A). With our present estimate of the total X-ray mass and the assumption that N103B is in the Sedov phase (i.e., that the ambient density is high), N103B could be the remnant of a Type I explosion with a low-mass progenitor. If the explosion occurred in a lower density medium, however, most of the mass must be stellar ejecta. Higher resolution spectral observations leading to an estimate of elemental abundances in the hot gas are needed to determine the remnant's type and present evolutionary phase.

VI. CONCLUSIONS

The X-ray spectrum of N103B, as measured with the ME + LE experiment aboard *EXOSAT* and the IPC experiment aboard the *Einstein Observatory*, clearly indicates a predominantly thermal source ($kT \sim 1.2$ keV) of X-ray emission. From the observed temperature, high X-ray luminosity, and small size of this SNR we derive an age of ~ 600 to 1200 yr and a high density inside and surrounding the remnant. Higher spatial and spectral resolution observations of N103B are required to determine the structure of its X-ray emission and to define precisely its dynamical and kinematical parameters.

We are glad to acknowledge the assistance of the *EXOSAT* observatory team.

REFERENCES

Becker, R. H., Helfand, D. J., and Szymkowiak, A. E. 1982, *Ap. J.*, **255**, 557.
 Davelaar, J., and Giommi, P. 1985, *EXOSAT Express*, **10**, 45.
 de Korte, P. A. J., *et al.* 1981, *Space Sci. Rev.*, **30**, 495.
 Giacconi, R., *et al.* 1979, *Ap. J.*, **230**, 540.
 Hamilton, A. J. S., Sarazin, C. L., and Chevalier, R. A. 1983, *Ap. J. Suppl.*, **51**, 115.
 Lampton, M., Margon, B., and Bowyer, S. 1976, *Ap. J.*, **208**, 177.
 Long, K. S., Dopita, M. A., and Tuohy, I. R. 1982, *Ap. J.*, **260**, 202.
 Long, K. S., Helfand, D. J., and Grabelsky, D. A. 1981, *Ap. J.*, **248**, 925.
 Masai, K. 1984, *Ap. Space Sci.*, **98**, 367.
 Mathewson, D. S., and Clarke, J. N. 1973, *Ap. J.*, **180**, 725.
 Mathewson, D. S., Ford, V. L., Dopita, M. A., Tuohy, I. R., Long, K. S., and Helfand, D. J. 1983, *Ap. J. Suppl.*, **51**, 345.
 Matsui, Y., and Long, K. S. 1985, in *Proc. Workshop on the Crab Nebula and Related Supernova Remnants*, ed. M. C. Kafatos and R. B. C. Henry (Cambridge: Cambridge University Press), p. 211.
 McKee, C. F., and Ostriker, J. P. 1977, *Ap. J.*, **218**, 148.
 Mills, B. Y., Turtle, A. J., Little, A. G., and Durdin J. M. 1984, *Australian J. Phys.*, **37**, 321.
 Osborne, J. 1985, *EXOSAT Express*, **13**, 42.
 Raymond, J. C., Cox, D. P., and Smith, B. W. 1976, *Ap. J.*, **204**, 290.
 Raymond, J. C., and Smith, B. W. 1977, *Ap. J. Suppl.*, **35**, 419.
 Smith, A., Jones, L. R., Peacock, A., and Pye, J. P. 1985b, *Ap. J.*, **296**, 469.
 Smith, A., Jones, L. R., Watson, M. G., Willingale, R., Wood, N., and Seward, F. D. 1985a, *M.N.R.A.S.*, **217**, 99.
 Turner, M. J. L., Smith, A., and Zimmerman, H. U. 1981, *Space Sci. Rev.*, **30**, 479.

D. J. HELFAND: Columbia Astrophysics Laboratory, Columbia University, 538 W. 120 Street, New York, NY 10027

H. W. SCHNOPPER and N. J. WESTERGAARD: Danish Space Research Institute, Lundtoftevej 7, DK-2800 Lyngby, Denmark

K. P. SINGH: Tata Institute of Fundamental Research, Homi Bhabha Road, Bombay 400005, India